# Reconstructing Contaminant Deposition in a San Francisco Bay Marina, California

**Adam H. Love**[1], **Bradley K. Esser**[2], and **James R. Hunt**[3]

[1]Postdoctoral Scientist, Environmental Science Division, Lawrence Livermore National Laboratory, P.O. Box 808, L-396, Livermore, CA 94551.

[2]Staff Scientist, Analytical & Nuclear Chemistry, Lawrence Livermore National Laboratory, L-231, Livermore, CA 94551.

[3]Professor, Dept. of Civil and Environmental Engineering, Univ. of California at Berkeley, 631 Davis Hall, Berkeley, CA 94720

## Abstract

Two sediment cores were collected from a marina in the San Francisco Bay to characterize historical sediment contamination resulting from the direct discharge of industrial wastewater from Naval Air Station Alameda. Depth profiles of trace metals, petroleum hydrocarbons, and radionuclides were determined with a 12-cm spacing down to a depth of 120 cm. The chronology of sediment accumulation is established by depth profiles of sedimentary time markers in conjunction with information on site history. The traditional approach of determining sediment accumulation rates by measuring atmospheric $^{210}$Pb deposition was obscured by a larger source of $^{210}$Pb in the sediments from the decay of anthropogenic $^{226}$Ra, likely from luminescent paints used at this facility and released to the marina. The sedimentation rates inferred from the data indicate that the greatest amount of contamination by trace metals and petroleum hydrocarbons took place between 1940 and 1960. In addition, anthropogenic $^{226}$Ra activities are positively correlated with some of the contaminants in the sediments, allowing the wastewater discharged from the facility to be distinguished from baywide contamination. In locations such as this, where there is a complex history of contaminant deposition, a source-specific tracer may be the only feasible method of attributing historical contamination to a point source.

### Keywords

Water pollution; History; Sediment; Metals; California; San Francisco; Hydrocarbons

## Introduction

Contaminated marine sediments are an important international problem that requires appropriate methods for site characterization and remediation. Contaminated sediments are typically found in estuaries near urban, industrial, and agricultural areas where fine-grained sediments accumulate. In general, the spatial extent of contamination is extensive while the vertical extent is limited. Two issues drive the need for characterization and remediation of contaminated sediment: the adverse impact on the ecosystem and the potential for contaminant

bioaccumulation into fish and shell-fish used for human consumption National Research Council (NRC 1997).

The San Francisco Bay has received wastes from municipal, industrial, agricultural, and mining activities that have altered the sediment quality (Hornberger et al. 1999). A recent study of the impact of human activities on sediments within San Francisco Bay (van Geen and Luoma 1999) demonstrated that historical contamination in Northern California was recorded chronologically in the sedimentary record. If sediment remediation is warranted, the contaminant depositional record must be deconvoluted into contaminants from both regional nonpoint sources and local point sources. This study characterizes the vertical distribution of contaminants in two sediment cores from a marina in the San Francisco Bay that is adjacent to industrial wastewater outfalls. Sedimentation rates in the marina are determined using natural and anthropogenic radionuclides $^{210}Pb$ and $^{137}Cs$ along with historical records. These rates are then used to reconstruct contaminant depositional histories. The contribution of contamination from local sources is distinguished from baywide contamination by identifying and correlating a component specific to local industrial operations. This study was part of a larger environmental investigation by the U.S. Navy to close the air station and return the facility to the local community (PRC Environmental Management, Inc. 1994; O'Day et al. 2000).

Krishnaswami et al. (1971), Koide et al. (1973), and Robbins and Edgington (1975) originally established the use of $^{210}Pb$ and $^{137}Cs$ to measure sedimentation rates in marine and lacustrine sediments. This technique was promptly applied to industrial pollution in the sedimentary record (Bruland et al. 1974; Edgington and Robbins 1976; Schubel and Hirschberg 1977; Goldberg et al. 1979). Many recent studies have incorporated this geochronological method to constrain the time of contaminant deposition (Bopp and Simpson 1989; Macdonald et al. 1991; Valette-Silver 1993; Krom et al. 1994; Gerritse et al. 1998; Palanques et al. 1998; Smith and Schafer 1999; van Geen and Luoma 1999; Yunker et al. 1999), but none distinguished specific point sources in complex depositional environments.

## Site History

The former Alameda Naval Air Station is one of many military bases that has closed and requires a site investigation prior to returning the facility to the local community. The Seaplane Lagoon is a marina within this facility at the western end of Alameda Island, adjacent to the city of Oakland as shown in Figs. 1(a and b). The rectangular marina was constructed in the 1930s on mudflats by the use of seawalls and dredging to a water depth of 6–7 m that reached into a consolidated sand formation called the Merritt Sand. The surface area of the lagoon is $4.5 \times 10^5$ m$^2$ and there is a 250-m-wide opening with access to San Francisco Bay. The marina is a site for sediment accumulation since it was dredged deeper than its preconstruction condition and is relatively protected from the currents and wind-generated waves in the larger bay system. Even so, there was no maintenance dredging required during facility operations. During the period 1943–1975 storm water and untreated industrial wastewater exclusively from the air station were discharged into the marina through seven outfalls indicated in Fig. 1(b). Use of $^{226}Ra$ to enhance night visibility of indicator needles, knobs, and deck markings began in the 1940s in the dial paint section of the instrument shop located in Building 5 treatment [Naval Energy and Environmental Support Activity (NEESA 1983)]. Normal operations in this building involved scraping old paint, cleaning with solvent, and repainting with paint containing $^{226}Ra$. Wastes from this location were discharged directly into the Seaplane Lagoon through the western outfall locations. The radium dial paint shop was closed in the late 1950s or early 1960s. Any refurbishing of radioluminescent paint was then performed on the second floor of Building 400 treatment (NEESA 1983). Between 1972 and 1975 the industrial wastewater from the whole facility was isolated and diverted for treatment (NEESA 1983).

The industrial wastewater plumbing system from Buildings 5 and 400 has been removed due to high $^{226}$Ra levels on the interior pipe surfaces.

## Experimental Methods

### Coring

In July 1997, two sediment cores were collected using a gravity corer near the wastewater outfalls at the northeast corner of the marina as indicated in Fig. 1. These two cores were separated by approximately 3 m. The gravity corer was 1.8 m long with a clear acrylic liner (9 cm internal diameter) and weighed 330 kg. Each sediment core was approximately 120 cm in length. Complete cores were collected because the sediment-water interface on the inside was the same as the mud level on the outside of the core barrel. In addition, the water above the sediment was not turbid, indicating no sediment loss by resuspension. Cores were maintained in a vertical position at all times during core acquisition and transport to shore. The cores were packed vertically in dry ice for 24 h until completely frozen to retain any semivolatile organic constituents and to prevent disturbance of the core during transport to the laboratory. Once in the laboratory, the cores were stored at $-15°C$ until they were sampled.

Both frozen cores were sectioned with a hacksaw into ten intervals, each approximately 12 cm deep. One core was used for radiologic analysis and bulk density determinations; the other was subsectioned for organic, metal, and bulk density determinations. Samples subsectioned for organic and metal analyses were approximately 9 cm in length; samples subsectioned for radiologic analyses were approximately 5 cm long; and bulk density profiles used subsections of approximately 2.5 cm. The frozen sediment was then extruded from the acrylic liner by hand and trimmed with a stainless steel surgical saw on all sides to avoid contamination from smearing during coring, sawing, and extrusion.

Dry bulk density was determined by gravimetric analysis after heating at $104°C$. Porosity was determined from the measured wet volume and mass loss of the wet sediment after drying, assuming all pore space was filled with water.

### Chemical Analysis

Samples for organic and metals analyses were kept frozen until they were thawed for extraction and analyses. The samples were homogenized over the depth interval of each sample. Methods for determining organic and metal concentrations in the sediment followed EPA guidelines (EPA 1996). The organic contaminants were extracted ultrasonically from the thawed sediment (3550A method). Total petroleum hydrocarbons (TPH) were measured using gas chromatography (8100 modified method). TPH were calculated from the gas chromatogram using Diesel No. 2 as the standard that most closely matched the hydrocarbon fingerprints in the samples. The metal contaminants were extracted from the thawed sediment by acid digestion (3050 method). The metals were measured using inductively coupled plasma–mass spectrometry (6020 method).

### Radionuclide Analysis

The activities of the radionuclides $^{40}$K, $^{137}$Cs, $^{226}$Ra, $^{228}$Ra, and $^{228}$Th were determined by gamma spectrometry using germanium solid-state detectors with a planar geometry. Details of the method are described by Wong et al. (1992); Bandong et al. (2001); and Volpe et al. (2001). $^{40}$K was quantified due to its association with clay minerals, $^{137}$Cs as a tracer of atmospheric weapons testing, and radium and thorium isotopes to examine natural and anthropogenic sources of other radionuclides in the sediment. A 60–100 g sample of freeze-dried sediment was hermetically sealed into an aluminum can and stored for 30–60 days to allow $^{222}$Rn (3.8-day half-life) and $^{214}$Pb (26.8-min half-life) to establish secular equilibrium

with $^{226}$Ra. Secular equilibrium occurs when the activities in a radionuclide decay series are equal. Samples were counted for 2–3 days in a low-level counting facility at Lawrence Livermore National Laboratory (LLNL) on calibrated detectors. Uncertainties (1 SD) from counting statistics, peak fitting, and line averaging were between 1 and 5%. With the exception of $^{137}$Cs, the nuclides mentioned were seen in every sample. Detection limits for $^{137}$Cs ranged from $8.3 \times 10^{-5}$ to $4.3 \times 10^{-4}$ Bq/g (0.005–0.026 dpm/g, where dpm indicates disintegrations per minute).

$^{210}$Pb activity was determined by isotope-dilution alpha spectrometry of its $^{210}$Po granddaughter. The details of the method are described by Benoit and Hemond (1988); Wong et al. (1992); and Ritson et al. (1994). The method assumes secular equilibrium between $^{210}$Pb and $^{210}$Po, which is reasonable for sediments. In preparation of marine sediments for analysis, a standard practice is to leach approximately 1 g of dry sediment in hot nitric acid after addition of a $^{209}$Po tracer, evaporate the leachate to dryness, reconstitute the residue in hydrochloric acid, and then deposit polonium onto a small silver planchet. The planchet is then alpha counted using partially depleted silicon surface barrier detectors, and the $^{210}$Po activity is determined from the measured $^{210}$Po/$^{209}$Po activity ratio. The uncertainty for the measurements is less than 6% (1 SD) and is dominated by counting statistics.

The normal technique for $^{210}$Pb determination was modified to remove the high concentration of refractory organic matter. One set of samples was dry ashed in a muffle furnace at 450°C (Krom and Berner 1983) and then leached in hot 1:3 hydrochloric:nitric acid. A second set of samples was leached in 1:3 hydrochloric:nitric acid and then wet ashed with hydrogen peroxide in concentrated nitric acid. Studies at LLNL (Wong et al. 1992) have shown that hot acid leaches quantitatively extract $^{210}$Po from marine sediments. Results from samples dry ashed were systematically low, indicating some loss of $^{210}$Po; therefore only $^{210}$Pb data from the wet-ashing protocol were considered.

## Results

Seaplane Lagoon sediment properties are not uniform throughout the recovered depth of 120 cm. The sediment was black fine-grained silty clay from 0 to approximately 90 cm below the sediment-water interface. From 90 cm to the bottom of the core the sediment rapidly graded into a gray silty sand of the Merritt Sand formation. There was no visual evidence of sediment reworking by benthic grazing organisms or benthic infauna. Bulk density and porosity are reported in Tables 1(a and b) for the two cores. Over the depth interval 0–90 cm below the sediment-water interface the dry bulk density is about 0.4 g/cm$^3$ and the porosity is about 75% in both cores. Since there is no evidence for compaction of the sediment over the depth interval of 0–90 cm, sedimentation rates are calculated as depth per time instead of reporting mass accumulation rates. The physical properties of the sediment were disturbed below 90 cm by the core retainer used to keep the sediment in the acrylic liner during sampling. Changes in sediment mineralogy can be discerned through $^{40}$K measurements since $^{40}$K is often used as a surrogate for clay content. The $^{40}$K activity at each measured interval (Table 2) from 0 to 90 cm below the sediment-water interface was 0.45±0.05 Bq/g (27±3 dpm/g). The uniformity in $^{40}$K activity and physical properties of the sediment indicates that there was no substantial change in sediment composition during the time period that deposited the upper 90 cm of sediment.

Chemical contaminants are not uniformly distributed over the sediment profile. Concentrations of five metals were measured within ten intervals and are plotted in Fig. 2 and included in Table 3. There were significant increases above surface sediment levels in Cd, Cr, and Pb from 39 to 85 cm below the sediment-water interface. Within this interval, Cd increased 14-fold, Cr increased two- to threefold, and Pb increased threefold above surface sediment levels. The

concentration of Cu and Zn increased slightly above surface sediment levels at depths of 35–65 cm. The concentration of Ni was below the quantitation limit of 85 mg/kg at every depth, while all other metals were significantly above the quantitation limit. The concentration of total petroleum hydrocarbons (Fig. 3 and Table 3) in the sediment varies from about 800 mg/kg in near surface sediments to levels as high as 4,200 mg/kg between the depths of 50 and 85 cm below the sediment-water interface.
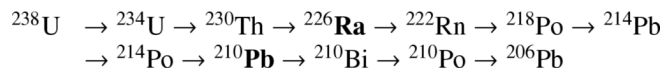
The activity profile of gamma-emitting radionuclides is shown in Fig. 4 and the data are presented in Table 2. The activities of $^{137}$Cs, $^{226}$Ra, $^{228}$Ra, and $^{228}$Th are normalized to the $^{40}$K variation using the following equation:

$$A_{\mathrm{norm}} = A_{(z)} \times A_{^{40}\mathrm{K(avg)}} / A_{^{40}\mathrm{K}(z)}$$

This normalization accounts for variations in radionuclide abundance associated with changes in clay content.

$^{137}$Cs is an anthropogenic radioactive isotope introduced into the global environment from fission reactions by atmospheric nuclear weapon testing. $^{137}$Cs has been deposited from the atmosphere into the sedimentary record since the inception of such activity in 1952 and fallout of $^{137}$Cs peaked in 1963. Since the position of the $^{137}$Cs maximum is at a sediment depth of 28±6 cm, this depth is a chronological marker for the year 1963 and suggests an average sedimentation rate of 0.8±0.2 cm/year from 1963 to 1997. The 6-cm uncertainty in the peak depth of $^{137}$Cs activity is attained from half the distance between sediment samples. The surface and near-surface $^{137}$Cs activities are comparable to activities measured elsewhere in the Bay (Fuller 1982; Fuller et al. 1999).

The radionuclides $^{226}$Ra and $^{210}$Pb are both constituents of the $^{238}$U decay series

$$^{238}\mathrm{U} \rightarrow {}^{234}\mathrm{U} \rightarrow {}^{230}\mathrm{Th} \rightarrow {}^{226}\mathbf{Ra} \rightarrow {}^{222}\mathrm{Rn} \rightarrow {}^{218}\mathrm{Po} \rightarrow {}^{214}\mathrm{Pb}$$
$$\rightarrow {}^{214}\mathrm{Po} \rightarrow {}^{210}\mathbf{Pb} \rightarrow {}^{210}\mathrm{Bi} \rightarrow {}^{210}\mathrm{Po} \rightarrow {}^{206}\mathrm{Pb}$$

The pronounced $^{226}$Ra maximum at 66 cm depth is anomalous compared to other San Francisco Bay sediment profiles (Fuller et al. 1999). Over the sediment depth intervals of 0–28 cm and 91–120 cm, the $^{226}$Ra activities are relatively constant and are similar to $^{226}$Ra activities found in other Bay sediments (Fuller et al. 1999). There are three possible reasons for enriched $^{226}$Ra within the core: (1) this sediment layer is mineralogically enriched in radium, (2) the sediment layer is mineralogically enriched in $^{238}$U, which then decays to $^{226}$Ra, or (3) there is an anthropogenic source of $^{226}$Ra.

The reason for $^{226}$Ra enrichment within the core is explained by examining other radionuclides over the sediment profile. If the sediment minerals are enriched in radium overall, the isotope $^{228}$Ra should also be enriched, but the $^{228}$Ra profile is uniform over the depth of the core. Thus, there is no enrichment in radium. The uniform composition of $^{228}$Ra and $^{228}$Th in the sediment also argues against an enriched U sediment source, since sediments enriched in U are often also enriched in Th because of geochemical similarities (Faure 1986). If U were the source for $^{226}$Ra, than these radioisotopes would be enriched in the sediment profile where $^{226}$Ra is elevated. Since neither a natural radium nor uranium source is indicated, the most likely source of the excess $^{226}$Ra in the Seaplane Lagoon sediment is anthropogenic. The historical record of $^{226}$Ra-based painting at this facility supports this analysis.

Sediment accumulation rates during the last 10–100 years are commonly determined by the $^{210}$Pb method. This method uses the natural deposition of $^{210}$Pb, but is complicated by

multiple $^{210}$Pb sources in the sediment. In a closed system, all of the $^{210}$Pb results from the $^{238}$U decay series. In contrast, sediments accumulate $^{210}$Pb from atmospheric and water column sources as well as production within the sediment. The $^{210}$Pb produced within the sediment is called "supported" and the $^{210}$Pb from other sources is called unsupported or "excess." The atmospheric source of $^{210}$Pb is from the decay of $^{222}$Rn and the water column contributes $^{210}$Pb from the decay of dissolved $^{226}$Ra. These additional $^{210}$Pb contributions to the sediments from the atmosphere and water column provide the excess $^{210}$Pb. Supported $^{210}$Pb is generally determined by measuring $^{226}$Ra activity in the core, assuming secular equilibrium, or by determining $^{210}$Pb activity at depth, where all excess $^{210}$Pb has decayed away. The excess activity of $^{210}$Pb is determined by subtracting the supported $^{210}$Pb from the total measured $^{210}$Pb. If the flux of atmospheric and water column $^{210}$Pb and the sedimentation rate are constant over time, a log-linear plot of excess $^{210}$Pb against depth in the sediment will yield a straight line as the excess $^{210}$Pb decays exponentially. The anthropogenic radium in the Seaplane Lagoon, a nonmineralogic contributor of $^{210}$Pb that presumably comes from World War II luminescent paint operations, obscures the excess $^{210}$Pb values by contributing $^{210}$Pb produced by the deposited paint. As a result, the atmospheric and water column excess $^{210}$Pb cannot be adequately distinguished from the $^{210}$Pb arising from the decay of anthropogenic $^{226}$Ra. Therefore, $^{210}$Pb is not useful in determining sediment accumulation rates at depth intervals containing anthropogenic $^{226}$Ra.

In light of these complications, supported $^{210}$Pb activities are estimated from the average of $^{226}$Ra in the upper 0–30 cm and bottom 90–120 cm sediment depths that are assumed not to contain significant anthropogenic $^{226}$Ra. This approach is justified by the close agreement of the $^{226}$Ra activity in these intervals, $1.7 \times 10^{-2}$ Bq/g(1.04 dpm/g), with $^{226}$Ra measured elsewhere in the bay. Excess $^{210}$Pb was then estimated by subtracting the average $^{226}$Ra from the measured $^{210}$Pb activities. Data are only available from three depth intervals in the sediment over depths from 0 to 30 cm below the surface as shown in Fig. 5. Excess $^{210}$Pb decays exponentially and was fitted to the simple sedimentation model

$$^{210}\text{Pb}_{\text{excess}} = {}^{210}\text{Pb}_{\text{surface}} \exp\left(-\lambda z / s\right)$$

(1)

where $^{210}\text{Pb}_{\text{surface}} = 3.0 \times 10^{-2} \pm 0.2 \times 10^{-2}$ Bq/g(1.8±0.1 dpm/g)=surface excess $^{210}$Pb; $\lambda$=decay rate constant for $^{210}$Pb ($3.09 \times 10^{-2}$ year$^{-1}$), $z$=depth; and $s$=sedimentation rate, determined to be 1.37±0.15 cm/year. This $^{210}$Pb-derived sedimentation rate is greater than the $^{137}$Cs-derived rate of 0.8±0.2 cm/year.

One method for evaluating the quality of the $^{210}$Pb data is to compare the flux of excess $^{210}$Pb to the sediment surface with other studies in the region. The excess $^{210}$Pb flux is determined by multiplying the surface excess $^{210}$Pb by the sedimentation rate and the bulk density. At the Seaplane Lagoon the excess $^{210}$Pb flux is 160 Bq/m$^2$/year (1.0 dpm/cm$^2$/year). This flux is five times higher than the local atmospheric fallout of 33 Bq/m$^2$/year (0.2 dpm/cm$^2$/year) (Fuller and Hammond 1983). Sediment focusing is commonly observed in estuarine sediments (Ivanovich and Harmon 1992), and a sediment $^{210}$Pb flux 15 times the atmospheric flux has been measured in Richardson Bay, approximately 20 km from the Seaplane Lagoon (Fuller et al. 1999). Within the larger San Francisco Bay system, in situ decay of $^{238}$U in the water column enhanced by exchange between bay waters and Pacific Ocean waters and the erosion within the drainage basin of soils containing excess $^{210}$Pb have been used to explain the elevated $^{210}$Pb flux results (Fuller 1982; Fuller et al. 1999). The Seaplane Lagoon is too shallow for in situ decay of $^{238}$U in the water column to be the dominant source of the additional $^{210}$Pb component. Input of additional $^{210}$Pb in sediment from the wastewater and storm water outfalls is the most likely source of the nonatmospheric component. The calculated surface $^{210}$Pb activity for the core is significantly lower than the baywide annual

average $^{210}$Pb activity in suspended sediment, $4.5 \times 10^{-2}$ Bq/g(2.7 dpm/g) (Fuller 1982), suggesting that wastewater and storm water outfalls may be the primary source of nonatmospheric excess $^{210}$Pb activity in lagoon sediments.

Two additional time markers can be used to determine sedimentation rates below sediment depths of 28 cm (1) The Seaplane Lagoon was dredged in 1935 into the Merritt Sand formation. In the sediment cores collected, the top of the Merritt Sand was located at approximately 90 cm depth, and (2) Significant radioactive fallout from atmospheric testing of nuclear weapons began in 1952, so the first appearance of $^{137}$Cs at 53 cm depth can be used as a chronological marker as well. Both of these time markers below 28 cm indicate a sedimentation rate of approximately 2.2 cm/year between depths of 90 and 28 cm below the sediment-water interface.

## Discussion

The $^{210}$Pb and the $^{137}$Cs methods for measuring sedimentation rates had a discrepancy in the results, and some justification is required in selecting one result over the other. Differences using these two methods are often the result of either bioturbation of the sediment or loss of the core top during sampling. Bioturbation would mix the greater surface activity of excess $^{210}$Pb with deeper sediments containing less $^{210}$Pb. As a result of bioturbation the calculated sedimentation rate is an upper limit. However, the effect of bioturbation is expected to be minimal since the sedimentation rate is relatively high (Olsen et al. 1981) and the high contaminant concentrations and anoxic conditions may deter biological habitation. If the core top was lost, the $^{137}$Cs-determined sedimentation rate would be higher than actual but there would be no change in the $^{210}$Pb sedimentation rate. If the upper 19±8 cm of the sediment profile were lost during sampling, then equal sedimentation rates would result from the $^{210}$Pb and $^{137}$Cs methods. There is no physical evidence for sediment loss during sampling, and the $^{137}$Cs estimate is more reliable than the $^{210}$Pb estimate due to uncertainty caused by the presence of luminescent-based paints. Nonetheless, if the $^{210}$Pb sedimentation rate is used for the years since 1963, the contaminant reconstruction changes very little because most of the contaminants were deposited prior to 1963.

The time period of contaminant deposition can be approximated using a sedimentation rate of 0.8 cm/year from the surface of the sediment to 28 cm, and 2.2 cm/year between 28 and 90 cm depth. The Cd, Cr, and TPH deposited within the sedimentary interval of 39–85 cm correspond with the years 1958–1938, where the highest levels at a depth of 62 cm represent 1950. The Cu profile is relatively uniform down to a sediment depth of 85 cm (estimated as 1938) followed by a decline at deeper depths. The Pb signature is uniformly high at 600 mg/kg over the sample depths of 39–73 cm corresponding to 1958–1944. The Zn deposited within the sedimentary interval of 39–62 cm corresponds with the years 1958–1950.

The lower metal concentrations at sediment depths of 0–27 cm appear to reflect the diversion and treatment of industrial wastewater from the lagoon outfalls in about 1974. The anthropogenic $^{226}$Ra peak corresponds to about 1944±4, which is consistent with the greatest industrial activity occurring during and after World War II. To demonstrate the degree to which these multiple lines of evidence are consistent, the sedimentary time markers, diversion of industrial wastewater, and peak of $^{226}$Ra are all plotted versus depth in Fig. 6.

Distinguishing the contribution of local sources of contamination from regional sources is often done by comparison with background locations. In some locations, such as the San Francisco Bay, sediment contamination is widespread and has fluctuated with altered industrial activities in the region. This precludes identification of a background level for comparison purposes. Therefore quantifying the contribution of site-specific sources is problematic.

In the Seaplane Lagoon one of the wastewater effluents contained a tracer, $^{226}$Ra, which is most likely unique to Naval Air Station operations. The anthropogenic contribution of $^{226}$Ra as a function of depth in the sediments is determined by using the $^{228}$Ra activity at that depth and the natural activity ratio of $^{228}$Ra/$^{226}$Ra to estimate natural $^{226}$Ra levels. Total $^{226}$Ra activity at a given depth minus the calculated natural $^{226}$Ra activity provides an estimate of the anthropogenic contribution. The uniformity of the $^{228}$Ra activity with depth and the reproducibility of the $^{226}$Ra/$^{228}$Ra ratio at depths where anthropogenic $^{226}$Ra is not evident both support this approach. Correlation of a contaminant with anthropogenic $^{226}$Ra suggests that the contaminant and $^{226}$Ra had similar release histories. Fig. 7 tests the correlation of the metals and TPH concentrations with the anthropogenic $^{226}$Ra activity. Total petroleum hydrocarbon, Cd, and Cr concentrations correlated with anthropogenic $^{226}$Ra activity and are likely from the same wastewater source or reflect similar levels of industrial activity at the base. Anthropogenic $^{226}$Ra activity and Pb, Zn, and Cu concentrations are not correlated. Although Pb has a distinct peak in the sediment, the lack of correlation with anthropogenic $^{226}$Ra may result from a contaminant source difference such as atmospheric deposition before leaded fuels were phased out for U.S. automobiles or spillage of leaded fuels from refueling of aircraft. The Zn data fluctuate in concentration with depth, but do not have a single distinct peak that correlates with anthropogenic $^{226}$Ra. Finally, no correlation of anthropogenic $^{226}$Ra with Cu should be expected since the Cu concentrations are relatively constant over the depth interval 0–90 cm where significant variations in $^{226}$Ra were observed.

The engineering profession needs adequate characterization of contaminated sediments prior to undertaking remedial activities. The sediment characterization methodology usually adopted by the maintenance dredging community is based on the collection of sediment cores and homogenizing them over intervals of meters since sediment removal operations will mix sediments over those depths. In contrast, the sediment chronologists are interested in the details of sediment accumulation and strive for sediment analysis over centimeter-depth intervals. Neither approach is practical for contaminated sediment sites that have spatial as well as depth variations. The use of 12-cm intervals in this study permitted determination of sediment accumulation rates and resolved contaminant releases over time intervals of decades. In addition, the ease of gamma counting minimizes sample handling and provides data on radionuclides for age dating, and in this case, identification of an anthropogenic source of $^{226}$Ra. This depth interval resolution was sufficient to assess the time periods when the majority of the contaminants were released into the marina. The approach could be easily extrapolated from a single location to a field site such as the whole marina without excessive analytical costs or modeling efforts.

## Conclusion

The composition, quantity, and vertical distribution of contaminants were characterized for only one location in an estuarine marina. Multiple lines of evidence arrived at average sedimentation rates and determined that the greatest contaminant loading was during or soon after World War II. These contaminants have been buried and there is no evidence for their presence in near-surface sediment. This one location is not representative of the entire marina since substantial horizontal heterogeneity was evident from earlier sampling efforts. The $^{226}$Ra in the sediments is specific to discharges from the Naval Air Station and can provides a unique opportunity to delineate the horizontal heterogeneity in contaminant distribution for a site with multiple sources of contamination. The data suggests that $^{226}$Ra measurements could be used as a surrogate for levels of some other industrial wastewater contaminants with a similar release history. Given the ease of $^{226}$Ra analysis, much greater spatial and depth distributions could be determined if warranted. These data suggest that vertical resolution of sediment contamination is essential in understanding historical discharges and current exposures. There is always a trade-off in the value of additional information and the cost of data acquisition that

must be addressed during each investigation. While this site has unique features, taking advantage of those features has been beneficial.

## Acknowledgments

## Notation

The following symbols are used in this paper:

| | |
|---|---|
| $A_{norm}$ | normalized radionuclide activity |
| $A_{(z)}$ | radionuclide activity at depth $z$ |
| $A^{40}K_{(avg)}$ | average $^{40}K$ activity |
| $A^{40}K_{(z)}$ | $^{40}K$ activity at depth $z$ |
| $^{210}Pb_{excess}$ | excess $^{210}Pb$ at depth $z$ |
| $^{210}Pb_{surface}$ | excess $^{210}Pb$ at sediment-water interface |
| s | linear sedimentation rate (cm/year) |
| z | depth (cm) |
| λ | $^{210}Pb$ decay constant (year$^{-1}$). |

## References

Bandong BB, Volpe AM, Esser BK, Bianchini GM. Pre-concentration and measurement of low levels of gamma-ray emitting radioisotopes in coastal waters. Appl. Radiat. Isot 2001;55(5):653–665. [PubMed: 11573799]

Benoit G, Hemond HF. Improved methods for the measurement of 210Po, 210Pb, and 226Ra. Limnol. Oceanogr 1988;33(6):1618–1622. part 2.

Bopp, RF.; Simpson, HJ. Contaminated marine sediments—Assessment and remediation. National Academy Press; Washington, D.C.: 1989. Contamination of the Hudson River: The sediment record.

Bruland KW, Bertine K, Koide M, Goldberg ED. History of metal pollution in southern California coastal zone. Environ. Sci. Technol 1974;8:425–432.

Edgington DN, Robbins JA. Record of lead deposition in Lake Michigan sediments since 1800. Environ. Sci. Technol 1976;10:266–274.

Environmental Protection Agency (EPA). Rep. No. SW-846. Washington, D.C.: 1996. Test methods for evaluating solid waste.

Faure, G. Principles of isotope geology. 2nd Ed. Wiley; New York: 1986.

Fuller, CC. PhD thesis. USC Sea Grant Institutional Program, Institute for Marine and Coastal Studies, Univ. of Southern California; Los Angeles: 1982. The use of Pb-210, Th-234 and Cs-137 as tracers of sedimentary processes in San Francisco Bay, California.

Fuller C, Hammond DE. The fallout rate of Pb-210 on the western coast of the United States. Geophys. Res. Lett 1983;10(12):1164–1167.

Fuller CC, van Geen A, Baskaran M, Anima R. Sediment chronology in San Francisco Bay, California by Pb-210, Th-234, Cs-137, and Pu-239,240. Mar. Chem 1999;64:7–27.

Gerritse RG, Wallbrink PJ, Murray AS. Accumulation of phosphorous and heavy metals in the Swan-Canning estuary, Western Australia. Estuarine Coastal Shelf Sci 1998;47:165–179.

Goldberg ED, Griffin JJ, Hodge V, Koide M, Windom H. Pollution history of the Savannah River estuary. Environ. Sci. Technol 1979;13:588–594.

Hornberger MI, Luoma SN, van Geen A, Fuller C, Anima R. Historical trends of metals in the sediment of San Francisco Bay, California. Mar. Chem 1999;64:39–55.

Ivanovich, M.; Harmon, RS., editors. Uranium-series disequilibrium: Applications to earth, marine, and environmental sciences. 2nd Ed. Clarendon; Oxford, England: 1992.

Koide M, Bruland KW, Goldberg ED. Th-228/Th-232 and Pb-210 geochronologies in marine and lake sediments. Geochim. Cosmochim. Acta 1973;37:1171–1187.

Krishnaswami S, Lal D, Martin JM, Meybeck M. Geochronology of lake sediments. Earth Planet. Sci. Lett 1971;11:407–414.

Krom MD, Berner RA. A rapid method for the determination of organic and carbonate carbon in geological samples. J. Sediment. Petrol 1983;53:660–663.

Krom MD, Kaufman A, Hornung H. Industrial mercury in combination with natural Pb210 as time-dependent tracers of sedimentation and mercury removal from Haifa Bay, Israel. Estuarine Coastal, Shelf Sci 1994;38:625–642.

Macdonald RW, Macdonald DM, Obrien MC, Gobeil C. Accumulation of heavy metals (Pb, Zn, Cu, Cd), carbon and nitrogen in sediments from Strait of Georgia, B.C., Cananda. Mar. Chem 1991;34:109–135.

National Research Council (NRC). Contaminated sediments in ports and waterways: Cleanup strategies and technologies. Washington, D.C.: National Academy Press; 1997.

Naval Energy and Environmental Support Activity (NEESA). Rep. No. NEESA-13-014. Calif.: Port Hueneme; 1983. Initial assessment study of Naval Air Station, Alameda, California.

O'Day PA, Carroll SA, Randall S, Martinelli RE, Anderson SL, Jelinski J, Knezovich JP. Metal speciation and bioavailability in contaminated estuary sediments, Alameda Naval Air Station, California. Environ. Sci. Technol 2000;34:3665–3673.

Olsen CR, Simpson HJ, Peng TH, Bopp RF, Trier RM. Sediment mixing and accumulation rate effects on radionuclide depth profiles in Hudson Estuary sediments. J. Geophys. Res., C: Oceans Atmos 1981;86:1020–1028.

Palanques A, SanchezCabeza JA, Masque P, Leon L. Historical record of heavy metals in a highly contaminated Mediterranean deposit: The Besos prodelta. Mar. Chem 1998;61:209–217.

PRC Environmental Management Inc.. *Ecological Assessment Draft Rep.* (17 February) and *Ecological Assessment Draft Report Amendment* (1 July). San Francisco: 1994.

Ritson PI, Esser BK, Niemeyer S, Flegal AR. Lead isotopic determination of historical sources of lead to Lake Erie, North America. Geochim. Cosmochim. Acta 1994;58(15):3927–3305.

Robbins JA, Edgington DN. Determination of recent sedimentation rates in Lake Michigan using Pb-210 and Cs-137. Geochim. Cosmochim. Acta 1975;39:285–304.

Schubel JR, Hirschberg DJ. Pb210-determined sedimentation rate, and accumulation of metals in sediments at a station in Chesapeake Bay. Chesapeake Sci 1977;18:379–382.

Smith JN, Schafer CT. Sedimentation, bioturbation, and Hg uptake in the sediment of the estuary and Gulf of St. Lawrence. Limnol. Oceanogr 1999;44:207–219.

Valette-Silver NJ. The use of sediment cores to reconstruct historical trends in contaminated estuarine and coastal sediments. Estuaries 1993;16(3B):577–588.

van Geen A, Luoma SN. The impact of human activities on sediments of San Francisco Bay, California: An overview. Mar. Chem 1999;64:1–6.

Volpe AM, Bandong BB, Esser BK, Bianchini GM. Radiocesium in North San Francisco Bay and Baja California coastal surface waters. J. Environ. Radioact 2002;60(3):365–380. [PubMed: 12054046]

Wong KM, Jokela TA, Eagle RJ, Brunk JL, Noshkin VE. Radionuclide concentrations, fluxes, and residence times at Santa Monica and San Pedro Basins. Prog. Oceanogr 1992;20:353–391.

Yunker MB, Macdonald RW, Goyette D, Paton DW, Fowler BR, Sullivan D, Boyd J. Natural and anthropogenic inputs of hydrocarbons to the Strait of Georgia. Sci. Total. Environ 1999;225:181–209. [PubMed: 10063650]
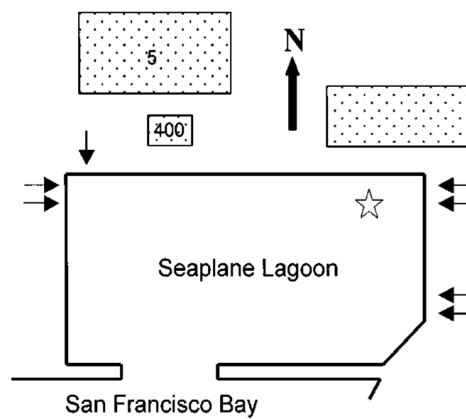
**Fig. 1.**
(a) Regional location of Naval Air Station Alameda and (b) diagram of Seaplane Lagoon. Arrows indicate location of wastewater outfalls. Star indicates sampling location. Relevant buildings are indicated by their building numbers
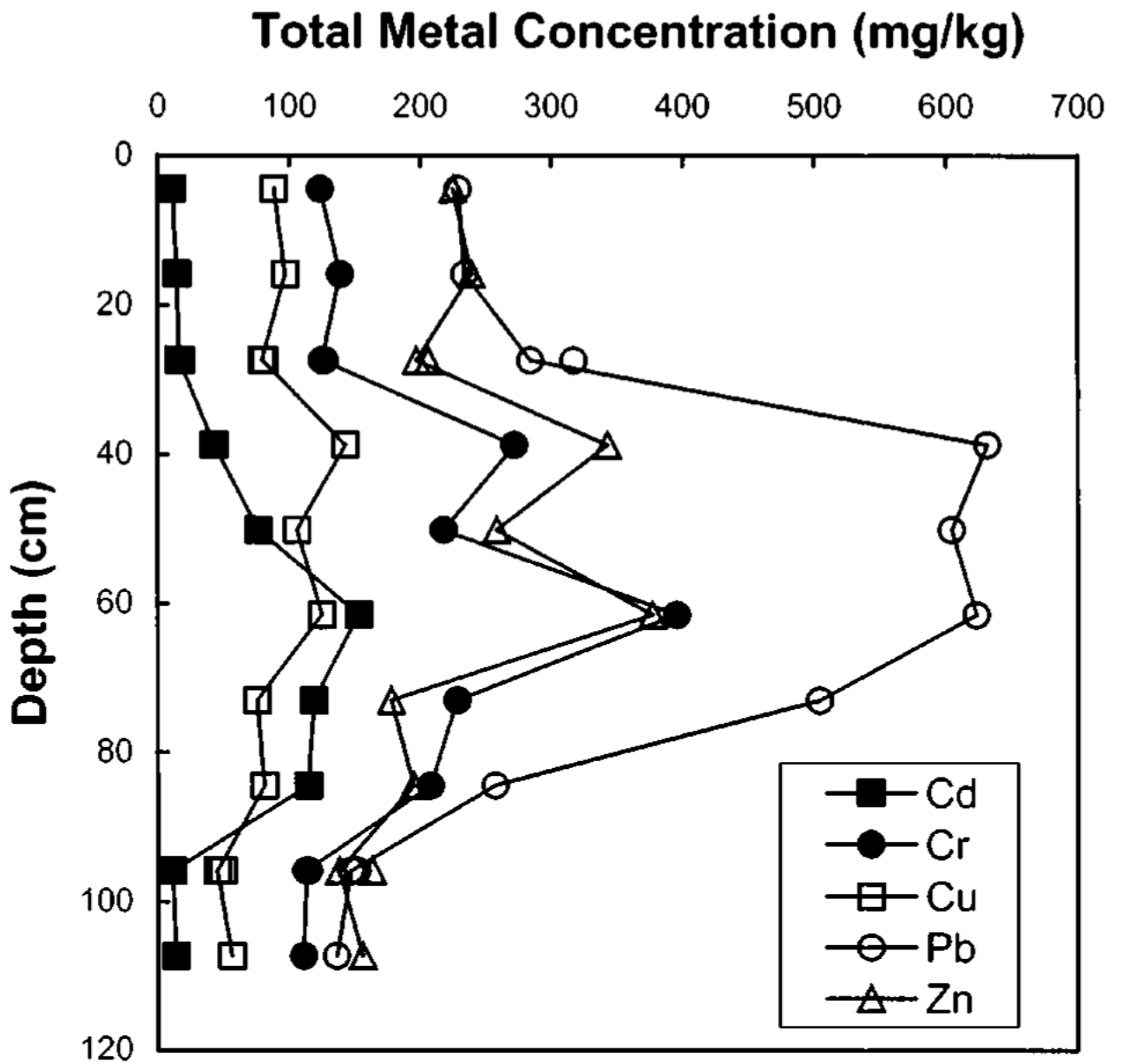
**Fig. 2.**
Depth profile of metal concentrations in Seaplane Lagoon sediment. Multiple points for each metal at 27 and 96 cm below sediment-water interface indicate duplicate measurements.
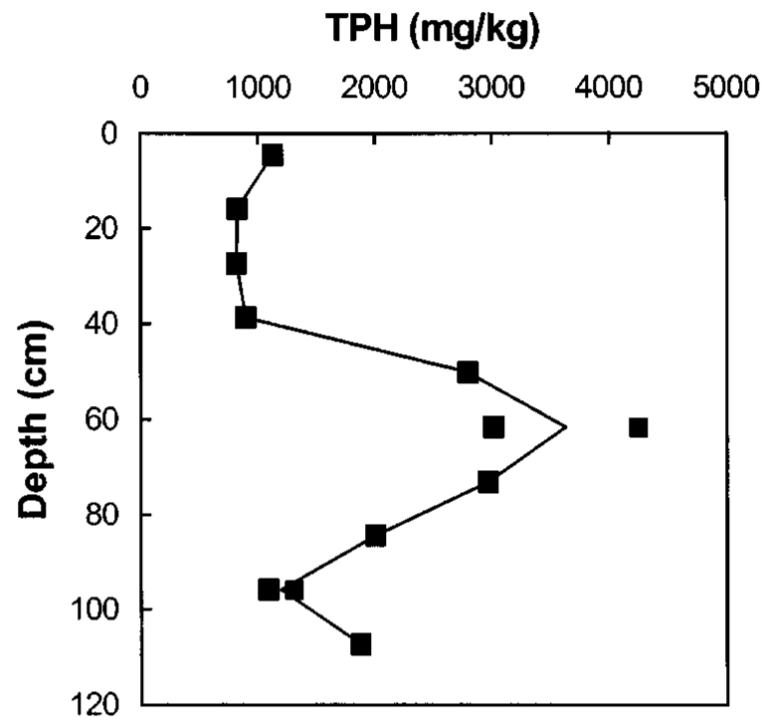
**Fig. 3.**
Depth profile of total petroleum hydrocarbons in Seaplane Lagoon sediment. Multiple points for TPH at 62 and 96 cm indicate duplicate measurements.
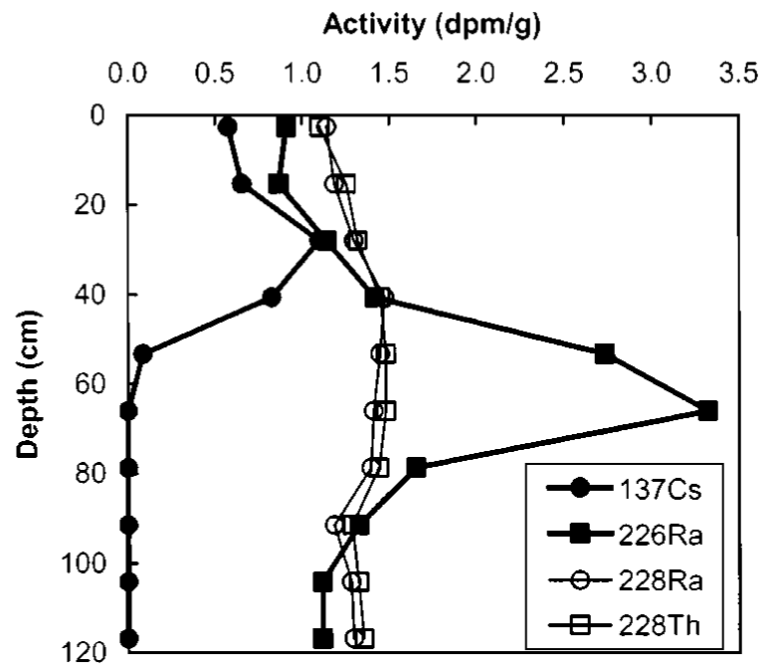
**Fig. 4.**
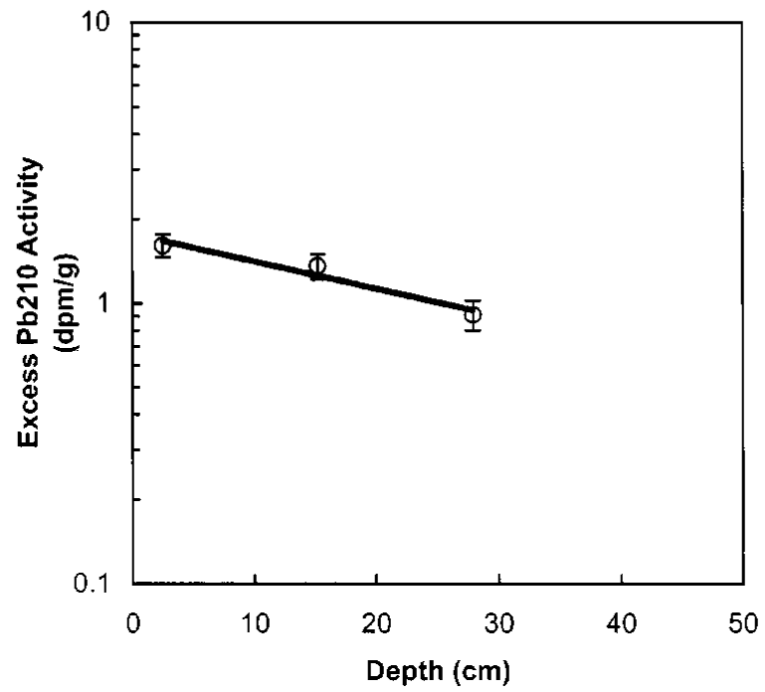Depth profile of gamma-emitting radioisotopes in Seaplane Lagoon sediment. Measurements normalized to $^{40}$K variation.

**Fig. 5.**
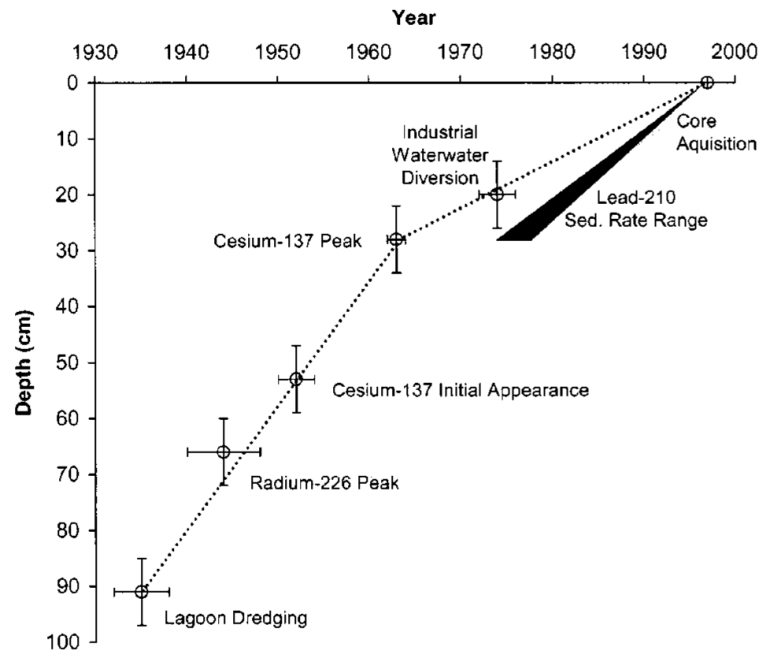Excess $^{210}$Pb activity versus depth in Seaplane Lagoon sediment

**Fig. 6.**
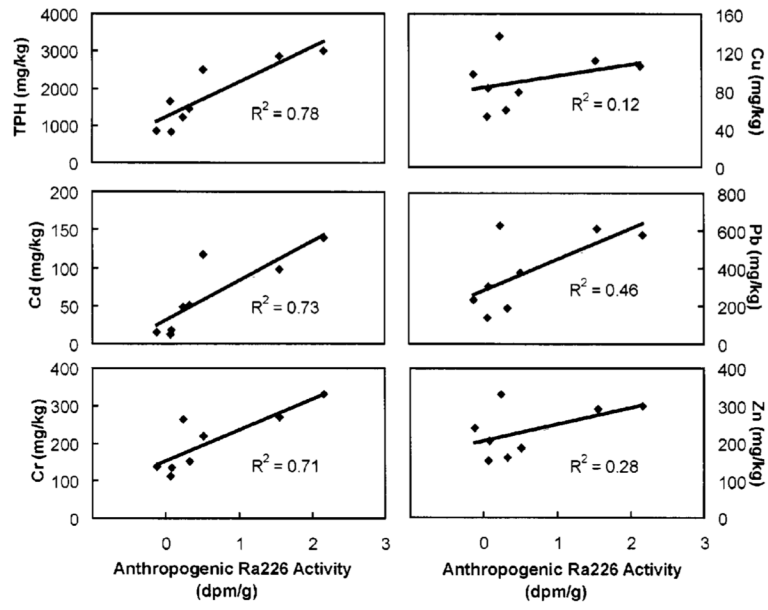Sedimentary time markers in sediment from Seaplane Lagoon

**Fig. 7.**
Correlation of calculated anthropogenic radium-226 activity with contaminants in Seaplane Lagoon sediment

**Table 1**

Sediment Bulk Properties

| Average depth (cm) | Sample interval (cm) | Dry bulk density (g/cm³) | Porosity (–) |
|---|---|---|---|
| (a) Isotope core | | | |
| 6.4 | 3.1 | 0.41 | 0.75 |
| 19 | 2.9 | 0.40 | 0.74 |
| 32 | 2.7 | 0.37 | 0.74 |
| 45 | 2.6 | 0.34 | 0.76 |
| 57 | 2.6 | 0.34 | 0.74 |
| 70 | 2.8 | 0.34 | 0.76 |
| 83 | 2.3 | 0.48 | 0.74 |
| 95 | 2.8 | 0.93 | 0.57 |
| 108 | 2.8 | 0.53 | 0.70 |
| 121 | 2.6 | 0.68 | 0.66 |
| (b) Organic and metals core | | | |
| 10 | 2.6 | 0.42 | 0.74 |
| 23 | 2.4 | 0.43 | 0.73 |
| 33 | 2.9 | 0.45 | 0.74 |
| 45 | 2.8 | 0.36 | 0.76 |
| 56 | 2.3 | 0.40 | 0.76 |
| 67 | 3.1 | 0.36 | 0.73 |
| 79 | 2.2 | 0.36 | 0.78 |
| 90 | 2.4 | 0.49 | 0.74 |
| 102 | 2.7 | 0.95 | 0.48 |
| 113 | 2.3 | 0.80 | 0.76 |

**Table 2**

Sediment Radionuclide Levels

| Average depth (cm) | Sample interval (cm) | $^{40}K$ (dpm/g) | $^{137}Cs$[a] (dpm/g) | $^{226}Ra$[a] (dpm/g) | $^{228}Ra$[a] (dpm/g) | $^{228}Th$[a] (dpm/g) |
|---|---|---|---|---|---|---|
| 2.5 | 5 | 30.6 | 0.58 | 0.91 | 1.14 | 1.10 |
| 15 | 5 | 26.1 | 0.65 | 0.87 | 1.18 | 1.25 |
| 28 | 5 | 31.0 | 1.10 | 1.14 | 1.30 | 1.32 |
| 41 | 5 | 28.0 | 0.83 | 1.41 | 1.47 | 1.45 |
| 53 | 5 | 22.7 | 0.09 | 2.73 | 1.45 | 1.48 |
| 66 | 5 | 24.8 | LT | 3.32 | 1.41 | 1.48 |
| 79 | 5 | 25.8 | LT | 1.65 | 1.39 | 1.44 |
| 91 | 5 | 23.9 | LT | 1.33 | 1.18 | 1.29 |
| 104 | 5 | 31.1 | LT | 1.11 | 1.28 | 1.32 |
| 117 | 5 | 24.0 | LT | 1.12 | 1.29 | 1.35 |

Note: LT indicates below detection limit.

[a]Normalized to $^{40}K$ variation

**Table 3**

Sediment Metals and Total Petroleum Hydrocarbon Concentrations

| Average depth (cm) | Sample interval (cm) | Cd (mg/kg) | Cr (mg/kg) | Cu (mg/kg) | Pb (mg/kg) | Zn (mg/kg) | Ni (mg/kg) | Total petroleum hydrocarbons (mg/kg) |
|---|---|---|---|---|---|---|---|---|
| 4.5 | 9 | 10.9 | 124 | 89 | 230 | 230 | LT | 1,130 |
| 16 | 9 | 15.0 | 139 | 98 | 230 | 240 | LT | 830 |
| 27 | 9 | 16.2 | 125 | 80 | 280 | 197 | LT | 820 |
|  |  | 17.5 | 127 | 81 | 320 | 210 | LT |  |
| 39 | 9 | 43 | 270 | 143 | 630 | 340 | LT | 900 |
| 50 | 9 | 77 | 220 | 106 | 600 | 260 | LT | 2,800 |
| 62 | 9 | 153 | 400 | 125 | 620 | 380 | LT | 3,600 |
|  |  |  |  |  |  |  |  | 4,200 |
| 73 | 9 | 119 | 230 | 76 | 500 | 178 | LT | 3,000 |
| 85 | 9 | 115 | 210 | 81 | 260 | 195 | LT | 2,000 |
| 96 | 9 | 11.3 | 113 | 45 | 147 | 138 | LT | 1,200 |
|  |  | 9.9 | 114 | 50 | 152 | 163 | LT | 1,300 |
| 107 | 9 | 13.6 | 111 | 56 | 136 | 156 | LT | 1,900 |

Note: LT indicates below detection limit.